# Analysis of CX3CR1 haplodeficiency in male and female APPswe/PSEN1dE9 mice along Alzheimer disease progression

Anne-Laure Hemonnot-Girard, Audrey J Valverde, Jennifer Hua, Charlene Delaygue, Nathalie Linck, Tangui Maurice, François Rassendren, Hélène Hirbec

Brain, Behavior, and Immunity 91 (2021) 404–417

Contents lists available at ScienceDirect

Brain Behavior and Immunity

journal homepage: www.elsevier.com/locate/ybrbi

# Analysis of CX3CR1 haplodeficiency in male and female APP$^{swe}$/PSEN1$^{dE9}$ mice along Alzheimer disease progression

Anne-Laure Hemonnot-Girard [a,b,1], Audrey J. Valverde [a,b,1], Jennifer Hua [a,b], Charlene Delaygue [a,b], Nathalie Linck [a,b], Tangui Maurice [c], François Rassendren [a,b], Helene Hirbec [a,b,*]

[a] IGF, Institut de Génomique Fonctionnelle, University of Montpellier, CNRS, INSERM, Montpellier, France
[b] Labex ICST, Montpellier, France
[c] MNDN, University of Montpellier, EPHE, INSERM, Montpellier, France

ARTICLE INFO

*Keywords:*
Alzheimer disease
Mouse model
Microglia
CX3CR1
Fractalkine receptor
Sex
Learning and memory
Glial reaction
Inflammation

ABSTRACT

Microglia, the resident immune cells of the brain, have recently emerged as key players in Alzheimer Disease (AD) pathogenesis, but their roles in AD remain largely elusive and require further investigation. Microglia functions are readily altered when isolated from their brain environment, and microglia reporter mice thus represent valuable tools to study the contribution of these cells to neurodegenerative diseases such as AD. The CX3CR1$^{+/eGFP}$ mice is one of the most popular microglia reporter mice, and has been used in numerous studies to investigate in vivo microglial functions, including in the context of AD research. However, until now, the impact of CX3CR1 haplodeficiency on the typical features of Alzheimer Disease has not been studied in depth.

To fill this gap, we generated APP$^{swe}$/PSEN1$^{dE9}$:CX3CR1$^{+/eGFP}$ mice and analyzed these mice for Alzheimer's like pathology and neuroinflammation hallmarks. More specifically, using robust multifactorial statistical and multivariate analyses, we investigated the impact of CX3CR1 deficiency in both males and females, at three typical stages of the pathology progression: at early stage when Amyloid-β (Aβ) deposition just starts, at intermediate stage during Aβ accumulation phase and at more advanced stages when Aβ plaque number stabilizes. We found that CX3CR1 haplodeficiency had little impact on the progression of the pathology in the APP$^{swe}$/PSEN1$^{dE9}$ model and demonstrated that the APP$^{swe}$/PSEN1$^{dE9}$:CX3CR1$^{+/eGFP}$ line is a relevant and useful model to study the role of microglia in Alzheimer Disease. In addition, although Aβ plaques density is higher in females compared to age-matched males, we show that their glial reaction, inflammation status and memory deficits are not different.

## 1. Introduction

Alzheimer Disease (AD) is a progressive neurodegenerative disorder and the most common cause of dementia worldwide. It mainly affects the elderly, with a much higher prevalence among women (Niu et al., 2017). The disease is characterized by different hallmarks including amyloid plaques, neurofibrillary tangles, neuroinflammation and, at advanced stages, brain atrophy (Bedner et al., 2015). Higher production and/or lower degradation of Amyloid-β (Aβ) fragments is thought to result in amyloid plaque formation, which represents one of the earliest and key events in AD pathogenesis. Transgenic mice harboring mutated human genes involved in the amyloid cascade provide valuable tools to study the disease progression (Esquerda-Canals et al., 2017). Among these models, the APP$^{swe}$/PSEN1$^{dE9}$ is one of the most popular as it recapitulates most of the important features of the disease (Jankowsky et al., 2004). It has been characterized at behavioral, histological and molecular levels in several studies (see https://www.alzforum.org/research-models/appswepsen1de9-c57bl6), however none of them have evaluated the effect of sex on disease progression using these multiple approaches.

Long considered as a consequence of the pathology, reactive glia and associated neuroinflammation are now regarded as playing key roles in AD initiation and progression. Indeed, human genetic studies identified over 25 genetic loci that robustly associate with AD risk (Hansen et al.,

* Corresponding author.
*E-mail address:* helene.hirbec@igf.cnrs.fr (H. Hirbec).
[1] These two authors contributed equally to the work.

https://doi.org/10.1016/j.bbi.2020.10.021
Received 6 July 2020; Received in revised form 2 October 2020; Accepted 21 October 2020
Available online 24 October 2020

2018; Verheijen and Sleegers, 2018). Among them, most genetic variants (Trem2, Ms4a genes, Picalm, etc.) code for proteins that are preferentially or exclusively expressed in microglia (Bellenguez et al., 2020). These findings strongly support a causal involvement of microglial cells in AD pathogenesis and generated a strong interest for studying these cells in AD (Cuello, 2017; Fan et al., 2017; Hampel et al., 2020; Nordengen et al., 2019). Yet, the roles of microglia in AD initiation and progression are unclear and heavily debated, with conflicting reports regarding their detrimental or protective contribution to the disease (for review see Takatori et al., 2019). Microglia are very sensitive cells that rapidly change morphology and function in-vitro, prompting the development of microglial reporter mice to study microglia in their natural environment (Gosselin et al., 2017).

CX3CR1 is a receptor for the chemokine Fractalkine/CX3CL1 whose expression is almost entirely restricted to myeloid cells. Heterozygous CX3CR1$^{+/eGFP}$ mutant mice which harbor a green fluorescent protein (eGFP) in the *cx3cr1* loci has become a valuable and widely used animal model to investigate microglial function (Jung et al., 2000). In most studies CX3CR1$^{+/eGFP}$ mice are used instead of WT and there are only few reports describing the impact of CX3CR1 haplodeficiency on the microglia functions or reactions (Maggi et al., 2011; Reshef et al., 2014; Rogers et al., 2011). However, CX3CR1-Fractalkine interactions regulate microglia homeostatic functions and is involved in many brain functions, including hippocampal neurogenesis (Reshef et al., 2014; Sellner et al., 2016), synaptic maturation (Arnoux and Audinat, 2015), microglia chemotaxis (Zhang et al., 2012), or neuronal survival (Zujovic et al., 2001). CX3CR1 signaling in microglia also constitutes an important regulatory mechanism by which neuronally-derived CX3CL1 restrains microglia overactivation during various inflammatory conditions (Wolf et al., 2013). Conflicting consequences of CX3CR1 partial and complete deficiency on cognitive functions have been reported (Maggi et al., 2011; Reshef et al., 2014). Unsurprisingly, CX3CR1 pathway is also altered in AD: fractalkine signaling is deficient in AD patient brains (Cho et al., 2011) and the CX3CR1-V249I variant has been associated with a higher neurofibrillary pathology progression (Lopez-Lopez et al., 2018). However, its exact role remains uncertain, as complete deletion of CX3CR1 has either neuroprotective or neurotoxic effects (for review Guedes et al., 2018). A few studies reported effects of CX3CR1 haplodeficiency on pathological features in AD mouse models but these studies were limited in terms of features and of co-factors evaluated (Hickman et al., 2019; Lee et al., 2010; Liu et al., 2010).

By crossing the APP$^{swe}$/PSEN1$^{dE9}$ (afterwards referred to as AD-C57) and CX3CR1$^{eGFP/eGFP}$ lines, we generated the APP$^{swe}$/PSEN1$^{dE9}$: CX3CR1$^{+/eGFP}$ line (afterwards referred to as AD-CX3) which represents a convenient model to study microglia during AD progression. Here, we validated this model by investigating in depth, whether CX3CR1 haplodeficiency has an impact on AD-like pathology progression. We analyzed the effects of this factor on cognitive behaviors, classic histological hallmarks of the disease (i.e. amyloid plaque burden, microgliosis and astrogliosis), as well as molecular changes (glial reaction and neuroinflammation). Impact of CX3CR1 partial deficiency may vary by stage of the disease or sex; the effects were thus evaluated in early, intermediate and advanced stages of the disease, in both males and females. Our findings confirmed that, compared to males, AD-C57 and AD-CX3 females display higher dense core plaques burden but we found that this is not associated with higher gliosis nor alteration of the neuroinflammation profile. Contrasting with the very recent study from Hickman et al. (Hickman et al., 2019), our findings indicate that CX3CR1 haplodeficiency has only limited impact on hallmarks of disease progression. Our analyses thus ascertain that APP$^{swe}$/PSEN1$^{dE9}$: CX3CR1$^{+/eGFP}$ mice provide a relevant model to investigate the role of microglia in Alzheimer Disease initiation and progression.

## 2. Results

### 2.1. Sex but not CX3CR1 haplodeficiency affects learning performances in APP$^{swe}$/PSEN1$^{dE9}$ mice

In AD-C57 mice, behavioral deficits emerge between 6 and 10 months of age and worsen with age (Minkeviciene et al., 2008). To measure the contribution of sex and CX3CR1 haplodeficiency in both AD and control (non-AD) mice on cognitive behavior, we assessed the visuo-spatial learning and memory in 12-months-old (mo) mice using the Morris water-maze test. Acquisition profiles were analyzed using a 4-way linear mixed-effects model (LMM) with sex (*Sex*), CX3CR1-haplodeficiency (*CX3-hdf*) and AD-status (*AD*) as between subjects' factors and training session (*Session#*) as within subjects repeated-measure factor. Regardless of the experimental group, all mice managed to learn the task (*Session#*: $p < 0.001$, LMM). Statistical analysis also revealed that after *Session#*, *Sex* was the factor that most affected the learning behavior (*Sex*: $p < 0.05$, LMM). Interestingly, sex seems to alter learning performances of controls but not AD mice (Figure-supp 2). Next analyses were thus performed separately on males and females using 3-way ANOVA (Fig. 1). In males, *AD* but not *CX3-hdf* has significant effects on the learning abilities with both AD-CX3 and AD-C57 mice showing learning deficits compared to their respective control littermates (Fig. 1C & 1E; *AD*: $p < 0.01$, LMM). There was also a significant contribution of the interaction between the 3 factors (i.e. *Session#*CX3*-hdf**AD*: $p < 0.01$, LMM) indicating that learning deficits are not strictly identical in AD-C57 and AD-CX3 male mice. Indeed, in the two last training sessions AD-CX3 mice performed better than AD-C57 (Fig. 1G). In females, only the *CX3-hdf* slightly affected the learning skills (*CX3-hdf*: $p < 0.05$, LMM); post-hoc analysis further revealed that this effect is mainly due to slightly better performances of controls-CX3 mice compared to their C57 counterpart (Fig. 1B).

Retention was tested 48h after the last training session, by assessing mouse ability to remember the location of the hidden platform. Results were analyzed using a 3-way LM model with *Sex*, *AD* and *CX3–hdf* as fixed factors. As sex did not significantly contribute to the model (*Sex*: $p = 0.683$, 3-way LM-model), results from both males and females were consolidated and analyzed using a 2-way ANOVA (Fig. 2A). As expected, contrary to controls, both AD-C57 and AD-CX3 mice did not properly discriminate the training quadrant, and meandered randomly in the pool (Fig. 2A-B). Two-way ANOVA post hoc analyses revealed that AD-CX3 mice performed significantly worse than their respective controls. The same trend was observed for C57 mice but difference did not reach statistical significance. Overall statistical analysis revealed that CX3-hdf did not affect mice memory (*CX3-hdf*: $p = 0.71$, 2-way ANOVA).

Of note similar results for learning and memory were obtained in the Barnes Maze test, another visuo-spatial memory test (Figure-supp 3A-E). These results were not due to altered exploratory behavior in AD mice as, on the opposite, we observed slightly increased locomotor activity in AD mice compared to controls in the open-field test (Figure-supp 3F; *AD*: $p < 0.05$, 3-way ANOVA; no difference in post hoc tests).

### 2.2. Sex and CX3CR1 haplodeficiency affect amyloid plaque load in a stage-dependent manner

Alzheimer Disease is characterized by specific histological and immuno-histological hallmarks. The most prominent feature, and a key pathogenic event in AD, is the presence of Amyloid-β (Aβ) deposits. To determine if *Sex*, *CX3-hdf* or interaction between these two factors alter AD-like pathology progression in APP$^{swe}$/PSEN1$^{dE9}$ mice, we assessed plaques burden in the cerebral cortex of 4-, 8- and 12-mo mice. Thiazine Red (TR) was used to quantify plaques area fractions (Fig. 3) and the plaques densities (Figure-supp 4) in all experimental groups. As expected, no significant TR staining was observed in control mice brains (Figure-supp 4A-C). In 4-mo AD-mice only very rare plaques were detected, but stage-dependent increase in the plaques area fraction and

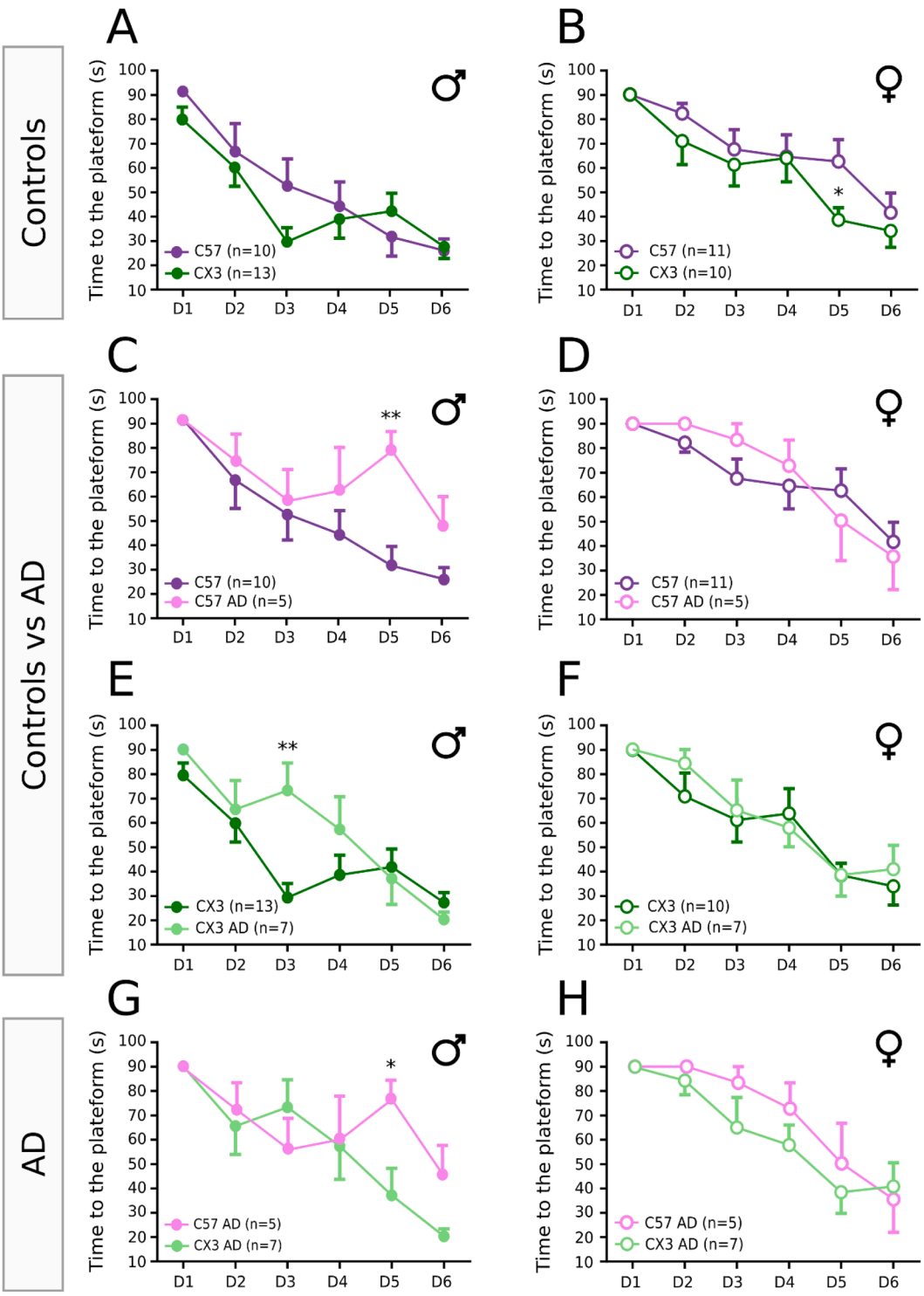


**Fig. 1.** In 12-mo mice, learning in the Morris Water Maze task is impacted by AD and to a much lesser extend by CX3CR1 haplodeficiency. Color code for the mouse genotypes are: C57BL6/J (C57; purple), APP/PS1:CX3CR1$^{+/+}$ (C57-AD; pink), CX3CR1$^{+/eGFP}$ (CX3; dark green) and APP/PS1:CX3CR1$^{+/eGFP}$ (CX3-AD; light green); plain and empty dots are for males and females respectively. Statistical analyses in males: 3-way ANOVA with *AD, CX3-hdf* as between subjects' factors and *Session#* as within subjects, repeated measures factor; *Session#*: $p < 0.001$; *AD*: $p < 0.01$; Statistical analyses in females: 3-way ANOVA with *AD, CX3-hdf* as between subjects' factors and *Session#* as within subjects, repeated measures factor factor; *Session#*: $p < 0.001$; *CX3-hdf*: $p < 0.05$. FDR corrected post-hoc tests; time point comparison: * $p < 0.05$, ** $p < 0.01$. Data are Mean ± SEM. (For interpretation of the references to color in this figure legend, the reader is referred to the web version of this article.)

density was observed in all experimental groups (Fig. 3A-B and Figure-supp 4D). Results from quantifications were analyzed separately in controls and AD mice. Three-way ANOVA confirmed the prominent importance of the *Age* factor for amyloid plaque load in AD-mice (*Age*: $p < 0.001$). *Sex* and *Cx3-hdf* did not affect the plaque load ($p > 0.05$ each), but there was a significant effect of the interaction between the three factors indicating that *Sex* and *CX3-hdf* affect plaque load differentially depending on the stage of the disease. In 4-mo mice, all AD mice

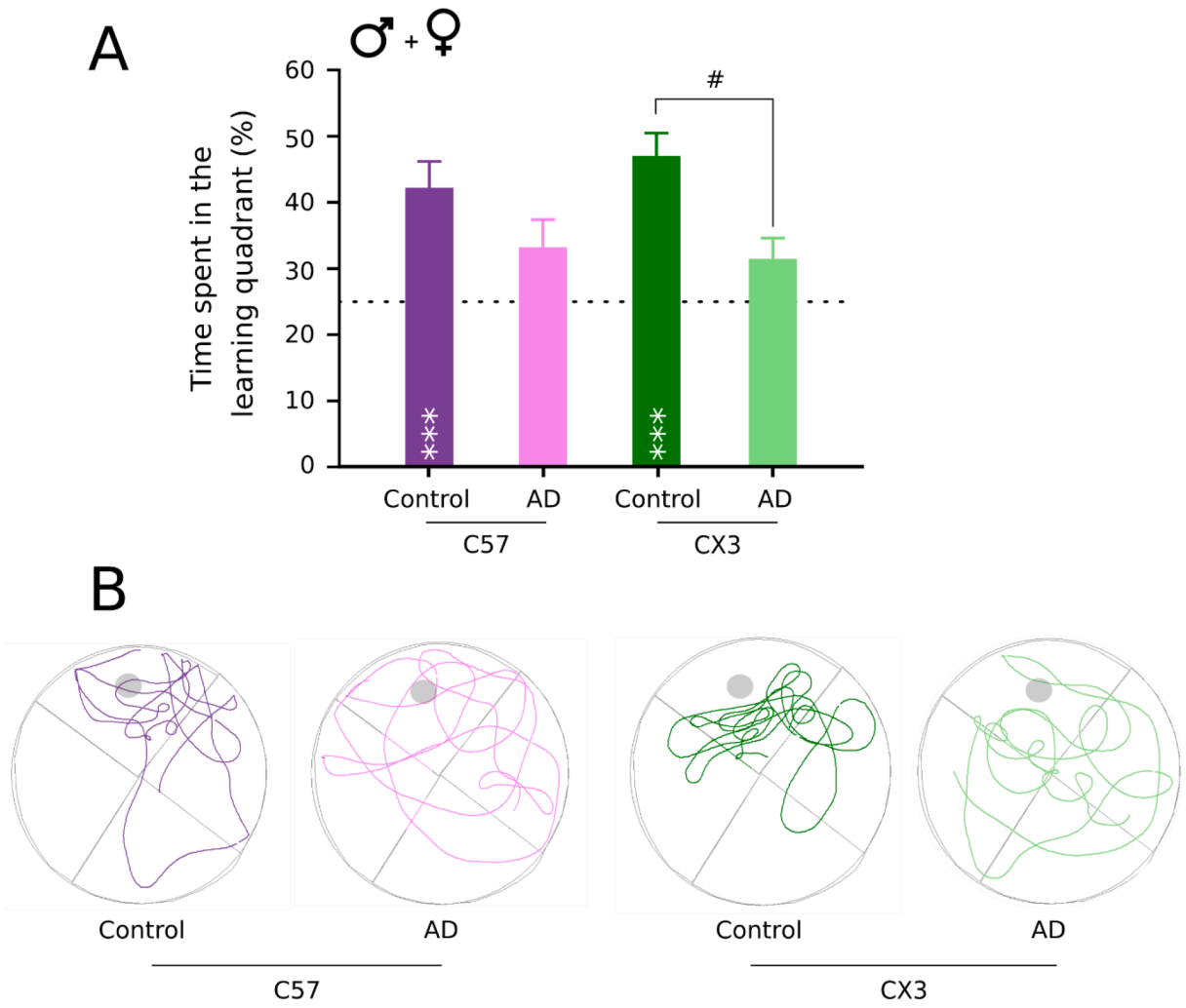


**Fig. 2.** 12-mo AD mice from both C57 and CX3 lines display memory deficit in the Morris Water Maze retention task. (A) Contrary to C57-AD (pink, n = 10) and CX3-AD (light green, n = 14), C57 (purple, n = 21) and CX3 (dark green, n = 23) control mice properly discriminate the learning quadrant. Data are Mean ± SEM. Statistical analyses for memory performance: Wilcoxon *t*-test: *** $p < 0.001$ compared to 25% theoretical value; Inter-group comparison: Two-way ANOVA with FDR corrected post-hoc tests: # $p < 0.05$. (B) Representative mice tracks during the retention task. (For interpretation of the references to color in this figure legend, the reader is referred to the web version of this article.)

presented the same plaque load. In contrast, 8-mo females displayed increased plaques load compared to males (*Sex*: $p < 0.001$; 2-way ANOVA on data in 8-mo mice), but, at this age, CX3-hdf factor did not alter this disease hallmark. Interestingly in these older mice, levels of soluble $A\beta_{1\text{-}40}$ and $A\beta_{1\text{-}42}$ was affected neither by sex nor CX3CR1 haplodeficiency (Figure-supp 4E) suggesting that higher plaques load in females is caused either by greater Aβ aggregation or increased Aβ production. In 12-mo mice, plaque load was affected by the interaction between *Sex* and *CX3-hdf* factors. It was increased in AD-CX3 male mice compared to their AD-C57 counterparts, while in females it was independent from CX3-hdf. Of note, we observed similar results for *Sex* or *CX3-hdf* effects in terms of disease progression over age, when measuring plaques densities (Figure-supp 4D).

### 2.3. Sex and CX3CR1 haplodeficiency have little impact on gliosis progression in $APP^{swe}/PSEN1^{dE9}$ mice

Increased microgliosis and astrogliosis are other important hallmarks of AD. To determine if CX3CR1 haplodeficiency and sex had any effect on microgliosis, we investigated microglial reaction by measuring IBA1 positive area fraction in mice cerebral cortex. Results from quantifications were analyzed separately in controls and AD-mice using 3-way ANOVA. In control mice, IBA1 area fraction was similar in males and females, was independent of CX3-hdf and remains stable until the mice are aged 12 months (Fig. 4A-B). In AD mice, no significant microglia reaction was detected at the early stage (i.e., 4-mo animals). However, from 8 months, we observed stage-dependent increase of microgliosis, with the *Age* factor displaying very significant effects (*Age*: $p < 0.001$; 3-way ANOVA; Fig. 4C-D). On the opposite, neither *Sex* nor *CX3-hdf* significantly contributed to the observed variance. Statistical analysis revealed a significant but dim interaction between the *Age* and *CX3-hdf* factors (*Age*CX3-hdf:* $p = 0.02$; 3-way ANOVA; Fig. 4D), with slightly increased microgliosis in 12-mo APP/S1:$CX3CR1^{+/eGFP}$ female mice compared to males.

In the cerebral cortex, homeostatic astrocytes express low levels of GFAP which remains almost undetectable by immunohistochemistry. Area fraction for this marker was used as a proxy to evaluate astrogliosis and to determine if age, sex or CX3CR1 haplodeficiency had any impact on astrocytes reaction. As for microgliosis, results from quantifications were analyzed separately in control and AD mice; 3-way ANOVA with *Sex*, *CX3-hdf* and *Age* as between subjects' factors were used. In control mice, GFAP immunoreactivity stayed globally stable across the ages. Statistical analysis revealed a dim effect of the interaction between the 3 factors (*Age*Sex*CX3-hdf*: $p = 0.016$; 3-way ANOVA) with slight

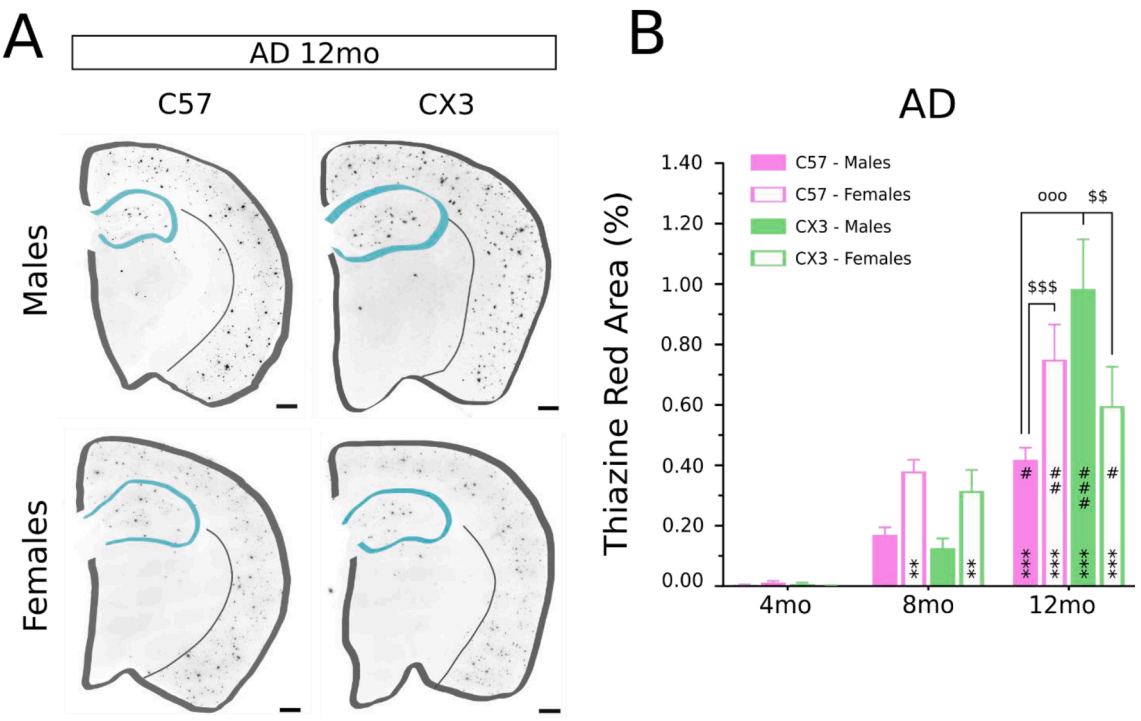


**Fig. 3.** Amyloid plaques load increase during AD progression: Sex and CX3CR1 haplodeficiency impact Aβ plaque load in an age/stage dependent manner. Representative Thiazine Red staining of 12-mo AD mice (A). Cortical and hippocampal contours are shown by grey and turquoise lines respectively, scale bar: 500 μm. Quantification of cortical Thiazine Red positive area (in % of total area) in AD mice (B) for both males (plain bars) and females (open bars) at the different ages. Data are Mean ± SEM. Statistical analyses: 3-way ANOVA with *Age*, *Sex*, *CX3-hdf* as between subjects' factors. AD-mice: *Age*: $p < 0.001$. FDR corrected post-hoc tests; compared to 4-mo: ** $p < 0.01$, *** $p < 0.001$; compared to 8-mo: # $p < 0.5$, ## $p < 0.01$, ### $p < 0.001$; *CX3-hdf* comparison: °° $p < 0.01$, °°° $p < 0.001$; sexes comparison: $$ $p < 0.01$. (For interpretation of the references to color in this figure legend, the reader is referred to the web version of this article.)

decrease in GFAP positive fraction in 12-mo females C57BL6/J compared to males (Fig. 5B). However, the contribution of this interaction to the global variance was <10%. Compared to control mice, 4-mo AD mice did not exhibit significant astrogliosis (Fig. 5D, analyses not shown). Increased astrogliosis was detected from intermediate stage (i.e., 8-mo mice) but stayed globally stable afterwards (*Age*: $p < 0.001$; 3-way ANOVA; Fig. 5D). Statistical analysis revealed that *CX3-hdf* had a significant (*CX3-hdf*: $p = 0.018$, 3-way ANOVA) but modest contribution (i.e., <5% of the global variance).

### 2.4. Sex and CX3CR1 haplodeficiency have little impact on the cortical neuroinflammation in $APP^{swe}/PSEN1^{dE9}$ mice

Microgliosis and astrogliosis occur late in AD progression. However, recent studies support that microglia and possibly astroglia reactions can arise already in the early AD stages. To determine if sex or CX3CR1 haplodeficiency could impact on the transcriptome remodeling in the cerebral cortex of AD-mice, we measured genes expression for 20 genes known to be deregulated under neurodegenerative conditions and/or specifically in AD. The majority of these genes are microglia specific and/or deregulated in reactive microglia (*Hexb, P2ry12, Ccl12, Ccl2, H2Aa, Cd68, Cd72, Cd86, Trem2, Tyrobp & Myd88*). We also included few neuroinflammation associated genes (*ApoE, Cxcl10, Il1b, Gfap & Tgfb*), as well as genes involved in APP processing (*Ctsd, Ide, Mme & Mmp9*). Gene expression changes and effects of *AD*, *Sex* and *CX3-hdf* fixed factors were analyzed individually at the different stages of the pathology using 3-way ANOVA. Complete results of these analyses are presented in Fig. 6 and Table S3. In addition, to get a global picture of gene expression changes we also performed complementary multivariate analyses at the different stages of the pathology.

In 4-mo mice, only few of the tested genes were significantly dysregulated. The most relevant effects (i.e., $p < 0.01$ and contribution to global variance higher than 15%) were an increased expression of *Cxcl10* in females but not males AD-mice and a decreased expression of *Mme* in controls $CX3CR1^{+/eGFP}$ mice. Consistent with these results, neither Principal Component Analysis (PCA) nor Agglomerative Hierarchical Clustering (AHC) managed to cluster the samples according to any of the fixed factor (Fig. 7A-B). Linear Discriminant Analysis (LDA) is complementary approach to PCA which focuses on maximizing the separability among known groups. Although samples tended to separate according to *Sex*, LDA also failed to clearly segregate the samples. In LDA analyses, cross-validation is a necessary step to determine the performance of a given predictive model, generated on a learning dataset, on new datasets. Here, two-fold cross validation indicated low model's performance as only 25% of the samples were correctly classified. As a whole, qPCR results indicated that, at 4-mo, genes expression are not affected by neither pathology, sex nor CX3CR1 haplodeficiency.

In 8-mo mice, pathology had significant impact on the expression of 60% (12/20) of the genes tested (Table S3) while *Sex* and *CX3-hdf* had much lower impact. Indeed, the most relevant effects were a slight decreased expression of both *Mme* and *Ide* in CX3CR1 haplodeficient mice. Consistent with these results, both PCA and AHC clustered samples in two groups corresponding to controls and AD mice (Fig. 7C-D), but none of these two analyses further discriminated for *Sex* nor *CX3-hdf*. PCA analysis revealed that leading genes for discriminating controls and AD samples are *Tgfb, Ctsd, Trem2, Gfap, Cd68* and *Tyrobp* (Fig. 7E). At this age, LDA clearly segregated controls from AD samples on the first component and there was also a trend for discrimination according to *CX3-hdf* on the second component. However, with about 35% of the samples with correct classification two-fold cross validation indicated low performance for this model (data not shown).

As expected, in 12-mo mice, *AD* factor affected the expression of almost all the genes we tested (17/20; Table S3). In contrast, *Sex* and *CX3-hdf* had no or little significant impact on gene expression.

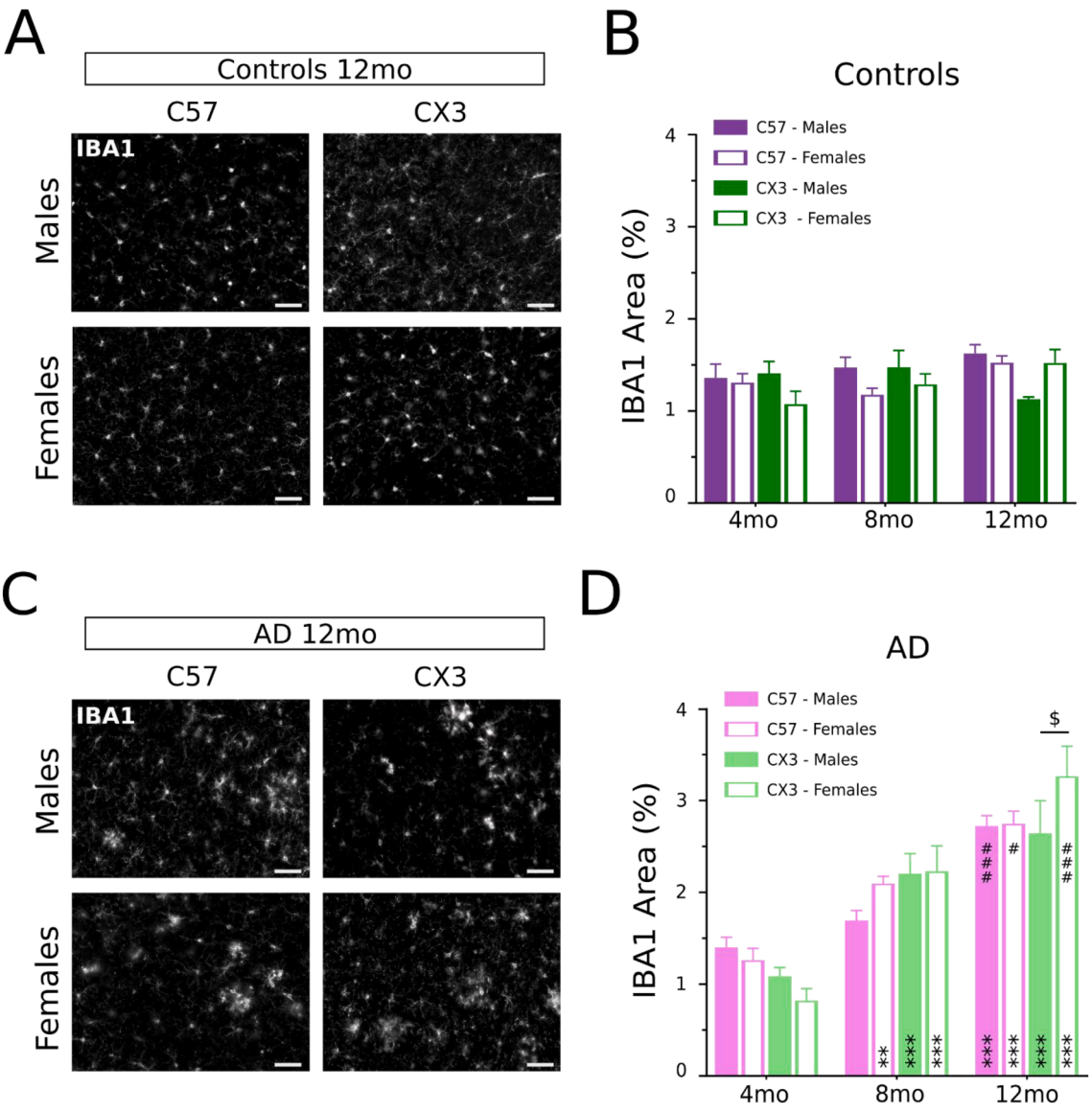


**Fig. 4.** Microgliosis increases during AD progression: sex and CX3CR1 haplodeficiency have little impact on the microgliosis in AD-mice. Representative IBA1 immunostaining in 12-mo control (A) and AD mice (C), scale bar: 50 μm. Quantification of cortical IBA1 fraction area in control (B) and AD-mice (D), for both males (plain bars) and females (open bars) at the different ages. Data are Mean ± SEM. Statistical analyses: 3-way ANOVA with *Age*, *Sex*, *CX3-hdf* as between subjects' factors. AD-mice: *Age*: $p < 0.001$. FDR corrected post-hoc tests; compared to 4-mo: ** $p < 0.01$, *** $p < 0.001$; compared to 8-mo: # $p < 0.05$, ### $p < 0.001$; sexes comparison: $ $p < 0.05$.

Accordingly, PCA and AHC appropriately segregated AD-mice from controls (Fig. 7F-G), but did not distinguish further for *Sex* and *CX3-hdf* factors. PCA analysis indicated that leading genes for discriminating controls from AD samples are *Cd68, Cd86, Cxcl10, Tyrobp, Gfap, Ctsd, Tgfb, Hexb* and *Ccl12* (Fig. 7H). Like PCA, LDA analysis segregated AD-mice from controls on the first component. However, two-fold cross validation indicated that the model led to a poor correct classification of the samples (i.e 30%). Of note we observed that, both in PCA and LDA, males AD-C57 samples tended to segregate from male AD-CX3 on the second component (i.e. plain pink dots versus plain green dots in Fig. 7F). However, the variance explained by the second component only represented 12.6% of the total variance and no specific gene could be associated with this discrimination.

As a whole, our qPCR analysis revealed that in early stage of the disease AD-like pathology, sex and CX3CR1 haplodeficiency have little impact on microglia reaction, neuroinflammation and pathways known to be altered in Alzheimer Disease. At more advanced stages, AD-like pathology leads to increased microglial response and neuroinflammation, but sex and CX3CR1 haplodeficiency have only very limited impact on this pathology driven features.

### 2.5. Complex impact of CX3CR1 haplodeficiency, age and AD-like pathology on the expression of Aβ degrading enzymes in $APP^{swe}/PSEN1^{dE9}$ mice

Brain Aβ levels are partly regulated by Aβ degrading enzymes, including Insulin Degrading Enzyme (IDE or Insulysin), Neprilysin (MME) and Metalloproteinase-9 (MMP9). Progression of AD has been associated with reduced expression of theses enzymes in microglia resulting in decreased Aβ degradation and increased accumulation of the Aβ peptide (Hickman et al., 2008; Miller et al., 2003). Recently, Hickman et al. (Hickman et al., 2019) reported higher expression of *Ide* and *Mmp9*, but not *Mme* in the brains of $APP^{swe}/PSEN1^{dE9}$:$CX3CR1^{+/eGFP}$ mice compared to that of $APP^{swe}/PSEN1^{dE9}$. We thus measured cortical RNA levels of the three enzymes and assessed the impact of the *AD*, *Sex* and *CX3-hdf* factors.

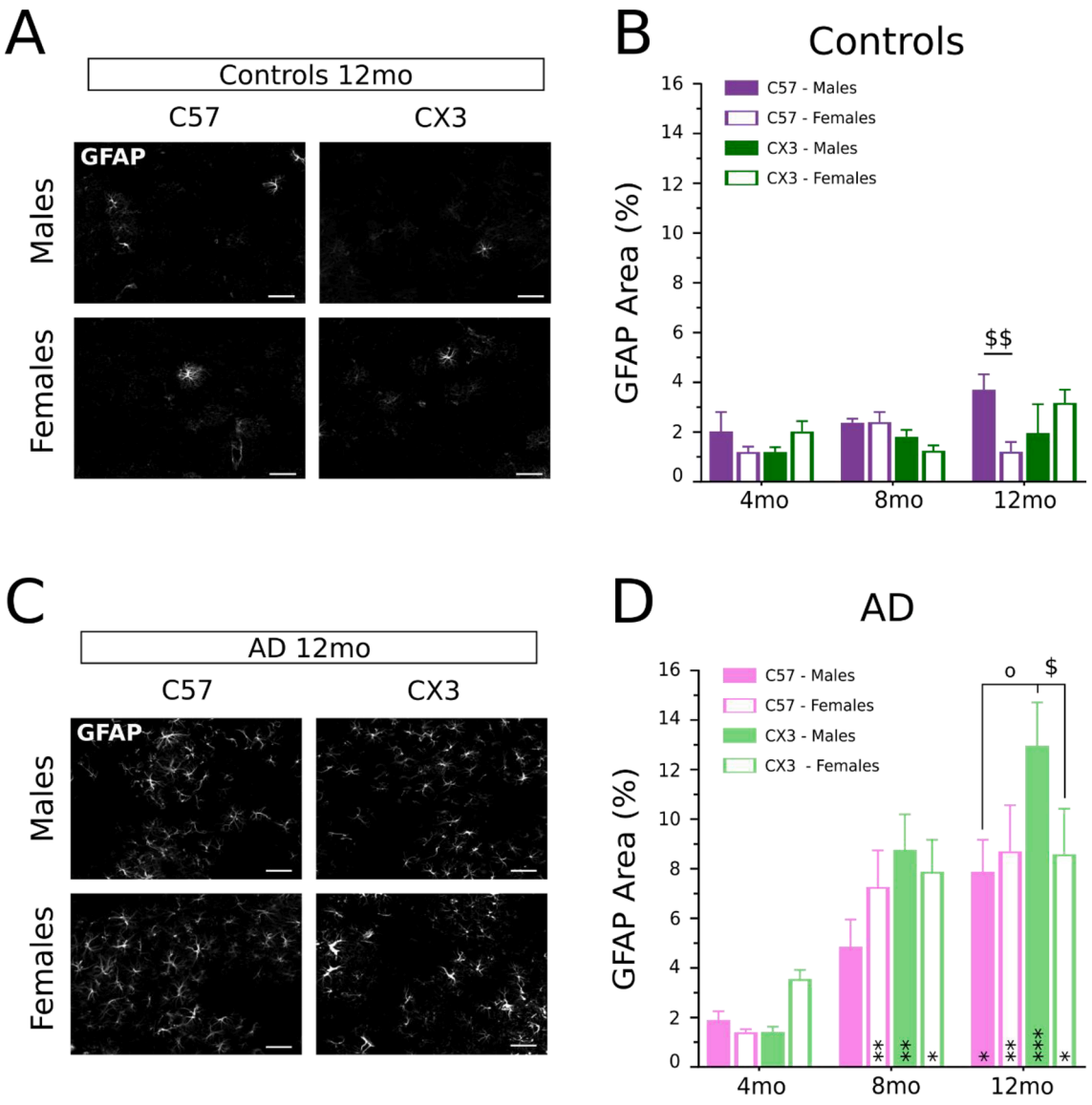


**Fig. 5.** Astrogliosis increases during AD progression: sex and CX3CR1 haplodeficiency have limited impact on the astrogliosis in AD-mice. Representative GFAP immunostaining in 12-mo control (A) and AD mice (C), scale bar: 50 μm. Quantification of cortical GFAP positive area (in % of total area) in control (B) and AD mice (D), for both males (plain bars) and females (open bars) at the different ages. Data are Mean ± SEM. Statistical analyses: 3-way ANOVA with *Age*, *Sex*, *CX3-hdf* as between subjects' factors. AD-mice: *Age*: $p < 0.001$; *CX3-hdf*: $p < 0.05$. FDR corrected post-hoc tests; compared to 4-month-old: ** $p < 0.01$, *** $p < 0.001$; sexes comparison: \$ $p < 0.05$; CX3-hdf comparison: 0 $p < 0.05$.

In contrast to Hickman's study and regardless of the mice age, we did not measure any significant reduction in *Ide* and *Mmp9* expression in the cortices of the AD-mice (Fig. 8A-F; Table S3). Our analysis also revealed that *Sex* did not impact significantly the expression levels of these two enzymes. However, in both 8- and 12-mo mice, we detected a decreased expression of *Ide* in CX3CR1 haplodeficient mice (Table S3; Fig. 8B-C).

Our results also indicated, in contrast to Hickman's results, a Sex and CX3-hdf independent decreased expression of *Mme* in 12-mo AD-mice (Table S3). Additionally, in 4-mo mice we measured higher *Mme* expression in controls CX3CR1$^{+/eGFP}$ mice compared to either C57 controls and AD-CX3CR1$^{+/eGFP}$ mice (Fig. 8G), while in 8-mo mice, CX3CR1 haplodeficiency led to AD independent *Mme* decreased expression. It should be noted that, although statistically significant, *Mme*'s expression varies at max by 30%. As a whole, these results suggest complex and tight CX3CR1, age and pathology dependent (but Sex independent) control of the expression of Aβ degrading enzymes in the brains of AD-57 mice.

## 3. Discussion

Numerous reports highlighted the importance of neuroinflammation in AD pathophysiology (Heneka et al., 2015), and recent GWAS and clinical imaging studies revealed its upstream role in the disease pathogenesis (Hampel et al., 2020). Microglia are the main immune cells in the brain. They play a key role in the immune surveillance of the brain parenchyma and initiate the inflammatory response when brain homeostasis is impaired, as it is the case when protein aggregates are formed. In AD, microglia are involved in both Aβ pathogenesis and in Tau pathology spreading (van der Kant et al., 2020) and thus represent an interesting therapeutic target. CX3CR1$^{+/eGFP}$ reporter mice provide useful tools to study microglia while preserving their *in vivo* physiological and pathophysiological functions. However, an important prerequisite to the use of this model is to demonstrate its relevance compared to the unaltered model. Here we provide a comprehensive study based on the assessment of multiple AD features (learning ability, histological hallmarks and neuroinflammation status), for both sexes

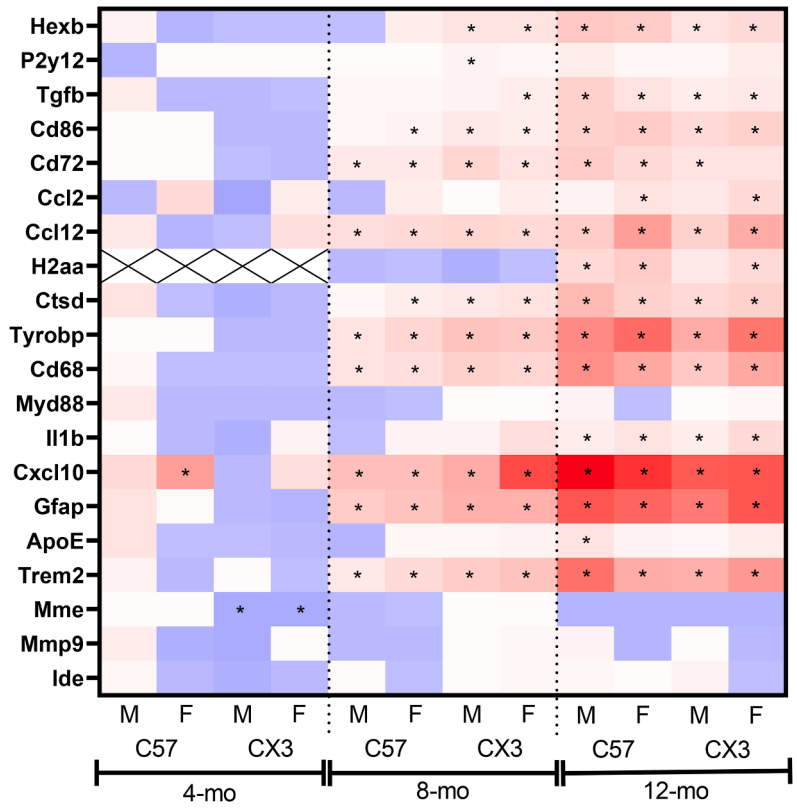


**Fig. 6.** Variation in the expression of selected genes across AD-like pathology. Heatmap showing expression fold-changes of selected genes. Genes were chosen from previous studies because they are (1) microglia specific and/or deregulated in reactive microglia (*Hexb, P2ry12, Ccl12, Ccl2, H2Aa, Cd68, Cd72, Cd86, Trem2, Tyrobp & Myd88*) (Hirbec et al., 2018; Keren-Shaul et al., 2017); (2) We also included few neuroinflammation associated genes (*ApoE, Cxcl10, Il1b, Gfap & Tgfb*) (Orre et al., 2014), as well as genes involved in APP processing (*Ctsd, Ide, Mme & Mmp9*) (Hickman et al., 2019). Statistical analyses: 3-way ANOVA FDR corrected post-hoc tests;*significant p-value compared to respective control.

and at different stages of the disease. It highlights the relevance of $APP^{swe}/PSEN1^{dE9}$:$CX3CR1^{+/eGFP}$ model to study the role of microglia in Alzheimer Disease initiation and progression.

AD is a progressive neurodegenerative disease that develops over years in humans and months in AD-mouse models. Recent data suggest that neuroinflammation, and microglia reaction in particular, occurs in two phases: an early phase, which initiates before cognitive deficits and is thought to have beneficial effects on the disease outcomes; and a second phase that contributes to increased neuroinflammation and neurotoxicity (Cuello, 2017; Fan et al., 2017). To our knowledge, our study is the first to present a thorough overview of the disease progression in $APP^{swe}/PSEN1^{dE9}$ mice (1) over different histological and molecular AD hallmarks, (2) in both sexes and (3) across three stages of the pathology. As attested by the absence of significant microgliosis, astrogliosis and change in the gene expression of a large range of inflammation related genes, our results demonstrate that in AD early stages, when plaques barely form, brain inflammation status is overall not different from that of control mice. As AD mice get older, hallmarks of the disease worsen: plaques burden increases in an age-dependent manner as do microgliosis and astrogliosis. Accordingly, we show an age-dependent increase of pro-inflammatory profiles in AD mice. This increase corresponds to both greater number of deregulated genes and stronger gene deregulation.

Sex effect in AD is well documented: prevalence is twice as high among women and higher longevity is not the only explanation (Hebert et al., 2013; Vina and Lloret, 2010). However, most AD pre-clinical studies use either males or females, but rarely both. In $APP^{swe}/PSEN1^{dE9}$, influence of sexual dimorphism was investigated in a handful of studies but they were mainly limited to mice at advanced stage of the disease (i.e., 12-mo or higher) and mainly focused on Aβ load (Gallagher et al., 2013; Janus et al., 2015; Jiao et al., 2016; Wang et al., 2003; Zhou et al., 2018). In parallel, a growing number of studies highlights the impact of sexual dimorphism on microglia functions (Bordeleau et al., 2019). In agreement with previous studies (Gallagher et al., 2013; Jiao et al., 2016; Wang et al., 2003), we confirmed that compared to males, female $APP^{swe}/PSEN1^{dE9}$ mice display greater plaques burden at both intermediate and advanced age but equal levels of soluble levels of $A\beta_{1-42}$ and $A\beta_{1-40}$. However, in contrast to Jiao et al. (Jiao et al., 2016), we found that higher plaques burden was not associated with increased gliosis. The weak effect of sex on the brain inflammatory status was confirmed by our transcriptomic analysis of a substantial number of inflammation related genes. Indeed, sex only affected the gene expression of a few genes, namely *Tyrobp* in 8- and 12-mo; *Cd86* in 8-mo and *Cd16* in 12-mo mice, and even for these few genes, impact on the global variance was weak (i.e., <10%). Additionally, the different multivariate analyses of our qPCR data failed to segregate males from females. Together, our results on plaques burden, soluble Aβ and neuroinflammation suggest that brain inflammatory status better correlates with soluble rather than aggregated Aβ concentration. This is consistent with data from the literature suggesting that non fibrillar soluble Aβ oligomers are more noxious than plaques aggregated Aβ fibrils (He et al., 2012). Effects of sex on learning impairment in $APP^{swe}/PSEN1^{dE9}$ mice have not been well documented and most studies either focused on one sex or males and females pooled in the same experimental groups (Janus et al., 2015). The most relevant study showed small deficits for 8/9-mo females $APP^{swe}/PSEN1^{dE9}$ in the Morris Water Maze reversal learning test (Gallagher et al., 2013), but no deficit in the training phase. Here we show that although both male and female quickly learned the task, learning abilities vary between males and females, with females showing a slower learning curve. Yet, we reveal spatial learning impairment in male but not female 12-mo AD-C57 mice. As for memory processes, they were not different in male and female controls and were similarly impaired in AD-C57 mice of both sexes. Overall, our data confirm the impact of the sex on the plaque load, but the lack of correlation between higher cortical Aβ deposition and neuroinflammation or behavioral deficits suggest that plaques load should not be used as a single marker to assess AD progression. Importantly, our study highlights the need to study progression of AD-like pathology in males and

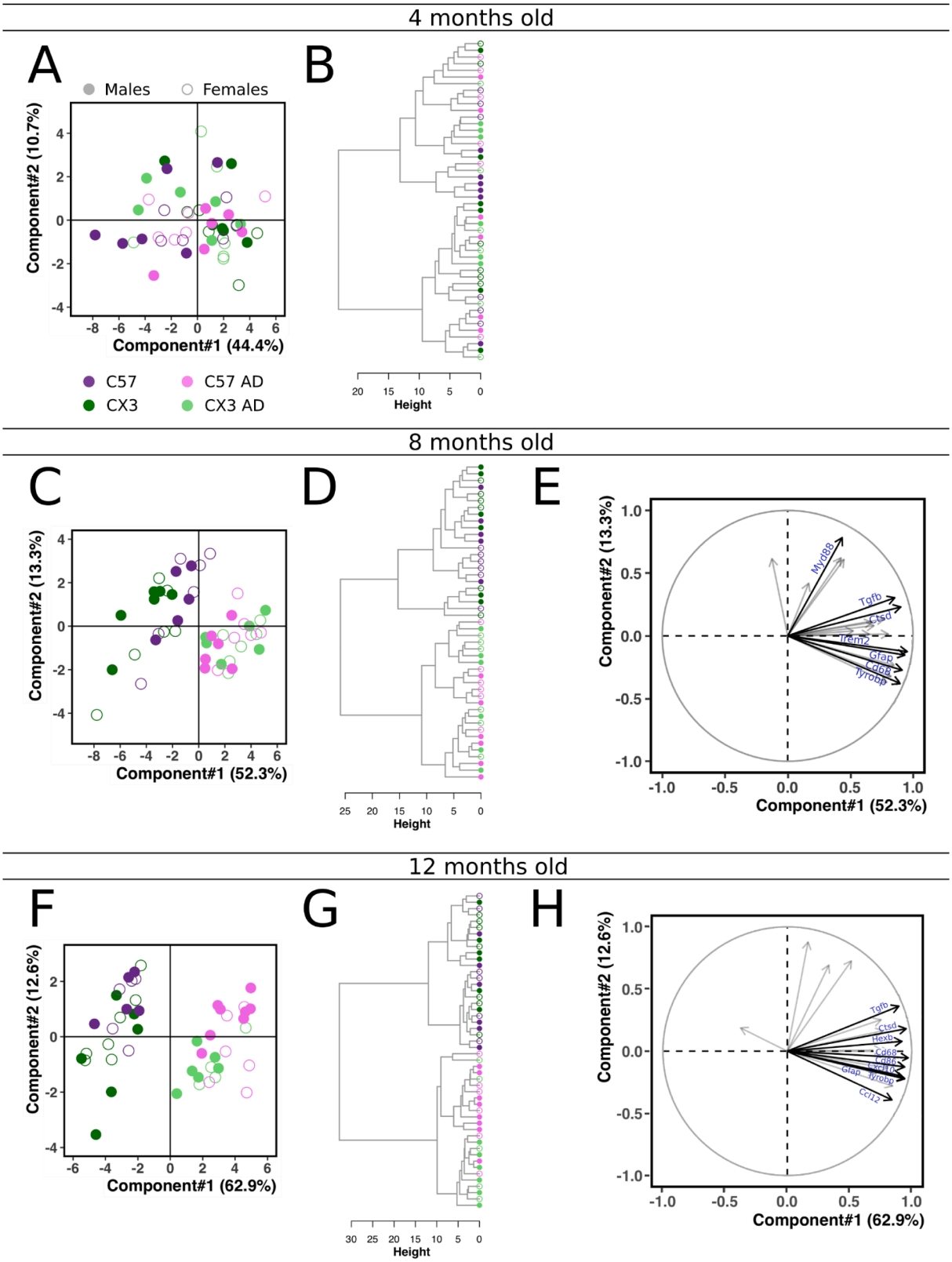


**Fig. 7.** Gene expression changes in the mice cortical homogenates for a range of inflammation and AD-related gens: Changes in gene expression were measured by qPCR in whole cortex, −ΔCq were calculated. Multivariate analyses were performed on −ΔCq. Gene expression is not significantly altered by sex, CX3CR1 haplodeficiency nor pathology in the early stage (A-B). In intermediate (C-E) and advanced (F-H) stages of the disease AD mice segregate from controls, but sex and CX3CR1 haplodeficiency does foster further segregation. In PCA, correlation circles allow identifying the most relevant variables for the separation of the observations on the different component/axes. Indeed, length of the vector, and closeness to the circle and the axe allows identifying the most relevant genes. In the present study, they (E-H) highlight the leading genes for segregation of AD versus control mice. Complete statistical results are given in Table S3. Included in these analyses are: Microglia related genes (*Hexb, P2ry12, Ccl12, Ccl2, H2Aa (except in 4mo), Cd68, Cd72, Cd86, Trem2, Tyrobp & Myd88*), neuroinflammation associated genes (*ApoE, Cxcl10, Il1b, Gfap & Tgfb*), and APP processing related genes (*Ctsd, Ide, Mme & Mmp9*).

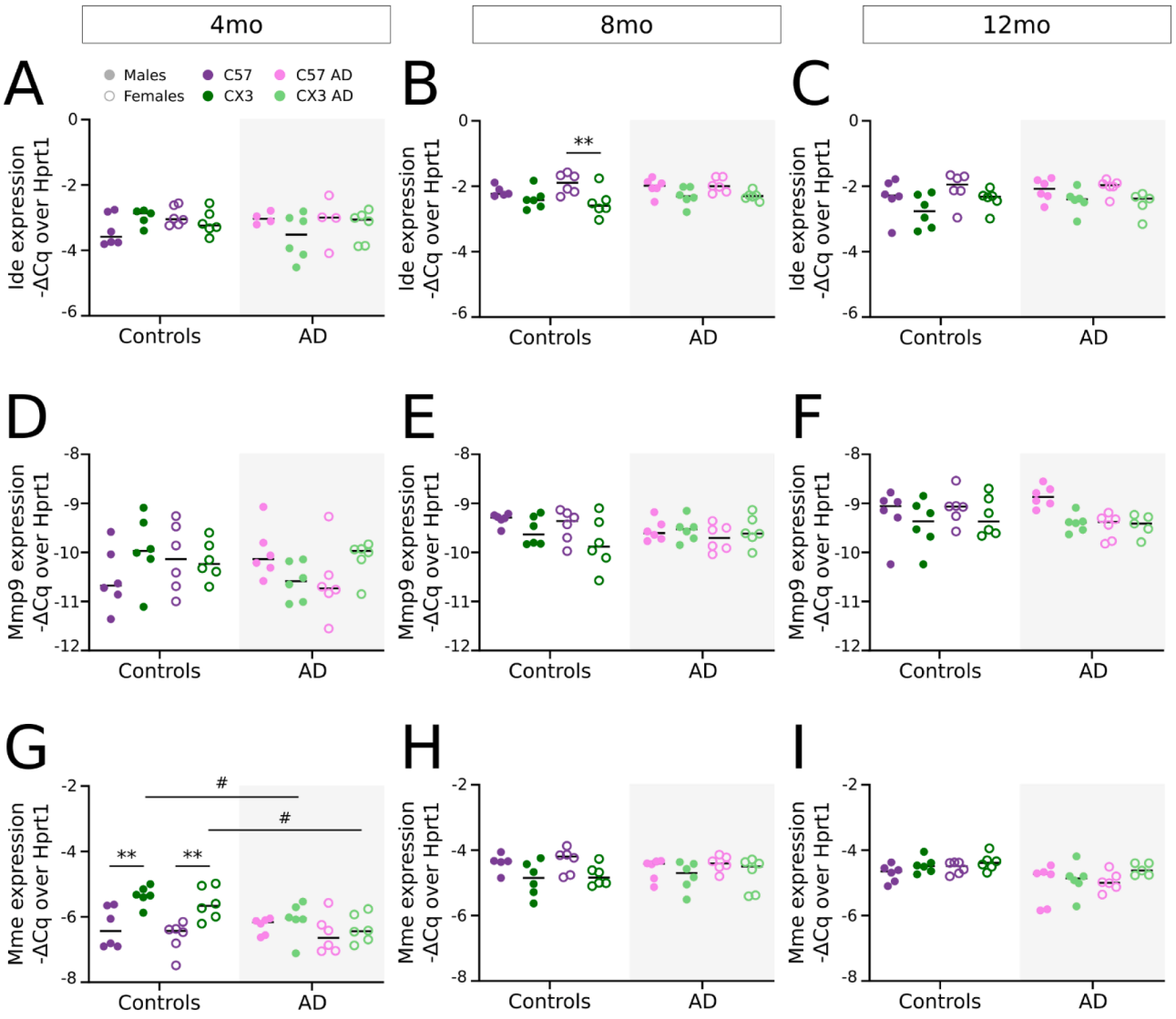


**Fig. 8.** *Ide*, *Mmp9* and *Mme*, APP degrading enzymes gene expression changes in mice cortical homogenates: Changes in gene expression were measured by qPCR in whole cortex and plotted as −ΔCq. Statistical analysis for each gene at every stage: 3-way ANOVA with *AD*, *Sex*, *CX3-hdf* as between subjects' factors. FDR corrected post-hoc tests; compared for AD status: # $p < 0.05$; CX3-hdf comparison: ** $p < 0.01$. Complete statistical results are given in Table S3.

females separately, using appropriate controls. The reason for higher plaque loads in female AD mice is currently unknown. Our qPCR analyses were limited to 20 genes and did not reveal any sex-difference in gene expression of Aβ degrading enzymes. Whether Aβ aggregation processes are increased in females, and whether microglia are involved in these processes remains to be explored. High-content approaches, such as RNA-seq, could be helpful in obtaining this information.

Our ultimate goal was to determine whether the $APP^{swe}/PSEN1^{dE9}$:$CX3CR1^{+/eGFP}$ mouse line could represent a relevant AD mouse model. To this purpose, we analyzed the impact of CX3CR1 haplodeficiency on AD progression. In AD mouse models, deletion of CX3CR1 had contrasting effects in different models: it reduced Aβ deposition, enhanced microglial Aβ phagocytosis and altered the neuroinflammation milieu in the APPPS1, R1.40 and CRND8 models (Lee et al., 2010; Liu et al., 2010), whereas in the hAPPJ20 and in the hTau models, it worsened the pathology by either increasing cytokine production (hAPPJ20; Cho et al., 2011) or Tau phosphorylation and aggregation (hTau, Bhaskar et al., 2010), and by exacerbating the behavioral deficits. Several AD mouse models have been crossed with the $CX3CR1^{eGFP/eGFP}$ line to investigate microglial functions in the context of AD (Baik et al., 2016; Gyoneva et al., 2016; Koenigsknecht-Talboo et al., 2008). However, only very few of these studies investigated the impact of haplodeficiency on the AD-like pathology progression (Hickman et al., 2019; Lee et al., 2010), and none explored its impact according to sex: Hickman's study focused on males, whereas in Lee's work the sex of the mice is not reported. At advanced disease stage, both studies described lower Aβ deposition in CX3CR1 haplodeficient mice, but results in terms of microgliosis, neuroinflammation and APP processing differs between the two studies. In agreement with Hickman et al. (Hickman et al., 2019), our learning and memory test analyses revealed slightly improved performance in 12-mo haplodeficient AD males compared to the AD-C57, with escape latencies similar to that of WT and $CX3CR1^{+/eGFP}$ mice in the two last training session. However, careful examination of the learning kinetics showed impairment for AD-CX3 in males compared to the appropriate controls. In our study, the slightly better cognitive performances of male AD-CX3 compared to males AD-C57 were associated with increase rather than decrease in plaques load and plaques densities. We also did not find any change in the expression of Insulin Degrading Enzyme (*Ide*) and Metalloproteinase-9 (*Mmp9*) genes in whole homogenates in either the AD versus controls, or $CX3CR1^{+/+}$ versus $CX3CR1^{+/eGFP}$ comparisons. Finally, we agree that CX3CR1 haplodeficiency does not affect microgliosis. The basis for the

contradictory results between our study and that of Hickman is not clear as the AD mouse models are similar (i.e. APP$^{swe}$/PSEN1$^{dE9}$ on C57BL6/J background). However, stages at which some of the analyses were performed (i.e. *Ide*, *Mme*, and *Mmp9* expression) may partly explain some of the differences observed. In addition, microglia are very sensible to their environment, and change in microbiota for example has been shown affect microglial transcriptome (Erny et al., 2017; Thion et al., 2018). Thus, it is possible that some difference in environmental parameters between the two labs could explain at least some of the observed discrepancies. Although individual gene expressions were modestly affected by CX3CR1 haplodeficiency in 12-mo male AD mice, multivariate analyses revealed a tendency towards segregation of males AD mice as a result of their CX3CR1 haplodeficiency. This suggested that, in older males, partial CX3CR1 deficiency may have a subtle impact on the pathology. Although it does not lead to higher plaques load, nor increased soluble Aβ concentration, astrogliosis or microgliosis, this interaction between sex and CX3CR1 haplodeficiency in 12-mo males AD mice correlates with higher expression of the *hAPP$^{swe}$* and *hPS1$^{dE9}$* transgenes in the males C57-AD mice. Importantly, in the younger mice of both sexes and in 12-mo females, our study demonstrates that CX3CR1 haplodeficiency do not significantly affect plaques load, neuroinflammation or APP processing in the APP$^{swe}$/PSEN1$^{dE9}$ model.

In summary, our study provides a comprehensive overview of the effect of the loss of one copy of the *Cx3cr1* gene on disease progression in the popular APP$^{swe}$/PSEN1$^{dE9}$ mouse model in both males and females. It reveals that, under our experimental conditions, CX3CR1 haplodeficiency does not significantly affect the evolution of the main hallmarks of the disease at early and intermediate stage of the pathology. The same is true at later stages in females. Overall, it demonstrates that the APP$^{swe}$/PSEN1$^{dE9}$:CX3CR1$^{+/eGFP}$ line is a relevant and useful model to study the role of microglia in Alzheimer Disease. In addition, our study provides useful comparison of the disease progression between males and females.

## 4. Methods

### 4.1. Animals

The APP$^{swe}$/PSEN1$^{dE9}$ mice used in this study co-express two genetic mutations associated with familial AD: a humanized amyloid precursor protein carrying the swedish mutation (APP$^{swe}$) and a mutant exon-9-deleted variant of the presinilin1(PS1$^{dE9}$). The APP and PSEN transgenes are integrated into a single locus and are expressed under the prion promotor (Jankowsky et al., 2004, 2001). These mice, thereafter referred to as APP$^{swe}$/PSEN1$^{dE9}$, were purchased from the Jackson Laboratories and subsequently bred in the SPF animal facility of the Institute for Functional Genomic (IGF, Montpellier, France; Agreement from the Ministry of Agriculture N° D34-172-13) to a C57BL6/J background. CX3CR1$^{eGFP/eGFP}$ mice were generous gift from Dan Littman (Jung et al., 2000) and are also maintained in the IGF facility under the C57BL6/J background.

To generate the genotypes used in this study, heterozygous APP$^{swe}$/PSEN1$^{dE9}$ male mice were crossed either with females C57BL6/J (purchased at Janvier Laboratories, France) or females $CX_3CR_1^{eGFP/eGFP}$, to obtain respectively APP$^{swe}$/PSEN1$^{dE9}$:CX3CR1$^{+/+}$ and APP$^{swe}$/PSEN1$^{dE9}$:CX3CR1$^{+/eGFP}$ mice, and their respective control littermates (i.e. C57BL6/J and CX3CR1$^{+/eGFP}$). For the sake of simplification, the different genotypes are referred to in the text and the figures as follows: C57/purple (C57BL6/J); CX3/Dark green (CX3CR1$^{+/eGFP}$), C57-AD/pink (APP$^{swe}$/PSEN1$^{dE9}$:CX3CR1$^{+/+}$) and CX3-AD/light green (APP$^{swe}$/PSEN1$^{dE9}$:CX3CR1$^{+/eGFP}$). C57 & CX3 are referred to as controls, and C57-AD & CX3-AD as AD-mice. Mice were housed in a 12 h light–dark schedule with food and water ad libitum. All experiments followed European Union (Council directive 86/609EEC) and institutional guidelines for the care and use of laboratory animals. The animal experiment protocols used in this study were approved by the Comité d'Ethique pour l'Expérimentation Animale Languedoc Roussillon (CEEA-LR; APAFiS#5252). Experiments were performed in 4-, 8- and 12-months-old (mo) animals. Males and females were used in parallel experiments. The experimenters were blind to group assignment.

The stability of expression of the endogenous *mApp* and *mPs1* genes *and* of the *hAPP$^{swe}$* and *hPS1$^{dE9}$* transgenes was tested for *Age*, *Sex* and *CX3-haplodeficiency* (*Cx3cr1-hdf*). Supplementary Fig. 1 shows that the expression of the endogenous *App* and *Ps1* transcripts is not affected by any of the factors. In 12-mo animals, statistical analyses revealed significant but small effects for some factors and interactions (i.e. representing <10% of the global variance). These were considered to be biologically irrelevant. Transgene expression was not affected by any of the factors in 4-mo animals, but 8-mo CX3-AD mice show slightly higher expression of *hAPP$^{swe}$* (*Cx3-hdf*: $p < 0.01$; 2-ways ANOVA; Fold Change (FC) = 1.25). On the contrary, in the oldest animals, expression of the transgenes was significantly higher in males, but not females, C57-AD mice (*hAPP$^{swe}$*: $p < 0.01$ post-hoc multiple comparisons, FC = 1.81; *hPs1$^{dE9}$*:, $p < 0.01$ post-hoc multiple comparisons, FC = 1.44). In CX3CR1$^{+/eGFP}$ mice, the expression of GFP is under the control of the Cx3cr1 promotor. In both 8- and 12-mo CX3-AD mice, the expression of the *Gfp* transcript was increased compared to the controls but this effect is probably due to the microgliosis observed at these ages.

### 4.2. Behavioral studies: Morris Water Maze

The Morris Water Maze allows testing long-term spatial memory. The mice were tested in a 140 cm diameter 40 cm height circular maze containing water at 20 ± 1 °C, opacified with lime carbonate. The light was adjusted to a non-aversive intensity of 80 lx. Fixed visual cues are displayed on distant walls around the maze for mice orientation. The protocol consisted of 6 days of learning during which mice had to locate and climb on an immerged platform always placed in the same quadrant, referred to as the training quadrant. For each trial mice started facing the wall from a randomly determined quadrant and were allowed to swim for 90 s. If the mice didn't reach the platform within the 90 s, they were gently placed on it for 20 s. Each mouse was given three trials per day with an inter-trial interval of 10 min. The escape time was calculated as the median latency of the three trials. The training phase was followed by a single probe test ("Retention test") performed 48 h after the last learning session, in the course of which the platform was removed. For the probe test, each mouse was allowed to swim once for 60 s. The trajectories were analyzed using videotracking (ViewPoint, Lissieu, France) and the time spent in each quadrant calculated. Mice failing to reach the platform at least once during the training sessions, whatever the experimental group, were discarded from the calculations. 10 mice over 78 were discarded accordingly (attrition 13%). Behavioral experiments were performed on 12-mo animals only. At least 5 mice were analyzed in each experimental condition, the numbers of mice are given in Table S1.

### 4.3. Tissue collection, preparation and staining

After induction of deep anesthesia with 2 μg/g pentobarbital (Euthasol Vet, TVM), the mice were perfused intracardially with 15 ml of phosphate buffer saline (PBS). For gene expression studies, the cortex was dissected, immediately frozen, and stored at –80 °C until use. For histological studies, the brains were fixed with 4% paraformaldehyde (PFA, Sigma Aldrich, P6148) for 2 h at room temperature (RT) and then overnight at 4 °C in fresh 4% PFA. Fixed brains were stored at 4 °C in PBS containing 0.1% Sodium Azide until they were cut into 40 μm sections using a Vibratome (Microm Microtec, Brignais, France).

*Thiazine Red Staining for Aβ plaques detection:* Thiazine red (TR) is an analog of naphthol-based azo structures which binds β-pleated sheet structures. Like Thioflavin-S, it stains dense core plaques but with maximum emission at 580 nm (Luna-Munoz et al., 2008). Vibratome floating sections were briefly washed with PBS and incubated for 5 min

at RT with 16 mg/L Thiazine Red (TR; Sigma Aldrich, S570435) in PBS. After a final rinsing session, sections were then mounted using Dako Fluorescent Mounting Medium (Dako, S3023) and stored at 4 °C until imaging.

*Immunohistochemistry:* Vibratome floating sections were incubated overnight at 4 °C with the appropriate primary antibodies: Rabbit-IBA1 (1:2000, Wako, MNK4428) or Rabbit-GFAP (1:500, Sigma Aldrich, G3893) diluted in 2% BSA, 0.1% Triton X-100, PBS Solution. Sections were then rinsed 3 times with PBS and incubated for 2 h at RT with Goat anti-Rabbit Cy3 secondary antibody (1:500, Jackson, 111–165-144). After a final rinsing session, sections were then mounted using Dako Fluorescent Mounting Medium (Dako, S3023) and stored at 4 °C until imaging.

### 4.4. Images acquisition, sampling and quantification

Slides were viewed using a classical epifluorescence microscope and images were acquired using an Imager Z1 microscope (Zeiss) equipped with an AxioCam MR R3 camera. Depending on the staining, 10X/0.3M27 Zeiss Plan-Neofluar (Thiazin-red) or 20X/0.50 M27 Zeiss Plan-Neofluar (IBA1 and GFAP staining) air objectives were used. The experimenters were blind to group assignment.

*Amyloid plaque load quantification:* For amyloid plaque detection, exposure time was maintained the same for all the acquisitions (ie: Cy3 30 ms). Images were acquired in mosaic mode at 10X magnification to visualize both cortical and hippocampal regions. Brain regions were delimited under CFP fluorescence, and the number of TzR positive deposits and the TzR positive area were quantified in the cortex and the hippocampus using a custom ImageJ macro. For the size of the particle, a threshold was set to skip particles smaller than 25 μm. The plaques were counted if they had a circularity between 0.2 and 1. 6 slices per animal were analyzed. At least 4 mice were analyzed in each experimental condition, the numbers of mice are given in Table S1.

*Microglial and Astrocyte quantification*: For analysis of IBA1 staining, for each field, 11 images (corresponding to 10 μm-thick optical sections) were acquired. For analysis of GFAP staining, for each field, 5 images (corresponding to 4 μm-thick optical sections) were acquired. In both cases, the exposure time was maintained constant (IBA1, 80 ms and GFAP, 30 ms). Stacked images were projected on the Z-axis and analyzed using a custom ImageJ macro to determine the percentage of immunopositive surface. For each animal, quantifications were performed in 4–5 randomly selected fields per section and 5 sections per animal. At least 4 mice were analyzed in each experimental condition, the numbers of mice are given in Table S1.

### 4.5. Gene expression studies

RNA from cortices were extracted using the Qiagen RNeasy Plus Mini kit (Qiagen, #74136) following manufacturer protocol. The quality of the total RNA was checked using the Agilent 2100 Bioanalyzer (Agilent). All RNAs had RNA Integrity Numbers (RINs) higher than 8.0. Reverse transcription of 500 ng total RNA were performed using the iScript kit (BioRad). Real-time PCR was performed in 384-well plates in a final volume of 10 μl using SYBR Green dye detection on the LightCycler480 system (Roche-Diagnostic). The primers pairs were designed using Primer 3 software. Lists of genes analyzed and primers sequences are given in Table S2. All analyzed genes showed detectable expression levels. *Hptr1* was selected as normalizing gene and we verified at each run that it is indeed expressed at similar levels in all groups. The results were expressed as Cq and normalized to the Cq value of the *Hptr1* (−ΔCq). At least 5 mice were analyzed in each experimental condition, the numbers of mice are given in Table S1.

### 4.6. Statistics

In the present study, we considered that only strong and medium effect sizes would be biologically relevant, i.e. only for strong and medium effect sizes, it would be possible to confer the factors or their interactions an impact on the characteristics of the disease. As a result, our experiments were designed to detect at least medium effect size of the different factors and/or their interactions. Thus, sample size was determined for an effect size of 0.4 and an expected power of 80%. Post-hoc analyses revealed that for factors and interactions with p-values comprised between 0.05 and 0.1, the actual effect size were $<0.3$, thus validating our conclusions regarding the lack of effect of any factor/interaction.

All data are presented as mean ± standard error of the mean (SEM). They were analyzed using General Linear Model procedures and were subjected to two-, three- or four-way ANOVA to determine significant main effects and interactions. Softwares used for statistical analysis were R (four-way ANOVA) or GraphPad Prism (8.4) (two- and three-way ANOVA). Post-hoc analyses for multiple comparisons were performed with Benjamini, Krieger & Yekutieli False Discovery Rate (FDR) corrections. In the Morris Water Maze probe test, time spent in the training quadrant was compared to the theoretical value of 25% using the Wilcoxon signed ranked test.

In gene expression studies, Principal Component Analysis (PCA), Agglomerative Hierarchical Clustering (AHC) and Linear Discriminant Analysis (LDA) multivariate analyses were performed using dedicated R packages. Missing data represented $<10\%$ of the datasets, for analyses they were imputed using the R missMDA package. P-values smaller than 0.05 were considered significant.

## 5. Supplementary procedures

### 5.1. Behavioral analyses

*Open-field:* Mice were tested in a white arena ($50 \times 50$ cm$^2$ and 45 cm height). The light was adjusted to a non-aversive intensity of 80 lx. The test consists of a single 10 min trial in which the mouse freely explores the environment. Analysis of trajectories was performed using the Videotrack® software (ViewPoint, Lissieu, France).

*Barnes Maze:* This test was used to assess spatial memory in a low stressful environment. The maze consists of a 120 cm elevated white flat circular platform (1 m of diameter) with 20 circular holes (50 mm of diameter) located equidistantly at the periphery of the platform. A hidden box located under one target hole allows the mice to escape from the platform. Fixed visual cues are displayed on distant walls around the maze for orientation. To motivate the mice finding the escape hole we used an aversive light stimulus of 370 lx and turned off the light as a reward. For each trial the mice were placed for 10 s in an opaque start box located in the center of the platform. To reduce mice stress, we performed a familiarization task 24 h prior to the first learning day. For the familiarization, after released from the start box, the mice were allowed to explore the maze once for 60 s and then gently placed in the hidden cage for 120 s with the reward. For the training trial, each mouse performed 4 trials per day with an inter trial interval of 15 min for 4 consecutive days. For each trial, after release from the start box, the mice were let to explore the maze for maximum 180 s. Trial was stopped when the mouse's four paws were in the target hole or when the maximum duration of the trial was reached. Mice that did not find the escape box within the 180 s were gently picked up and moved to the target hole, into the escape box. Mice were left in the escape box with the lights off for 60 s before being returned to their home cage. 72 h after the fourth training session we performed the retention test where the hidden cage was removed. We let the mice explore the maze once for 90 s and then returned to their home cage. The platform surface and holes were carefully cleaned with 20% ethanol solution and distilled water between each trial to remove any olfactory cues. All trials were recorded with an automated videotracking software (Ethovision® XT13, Noldus). Primary error (number of wrong pokes before poking the target hole), primary latency (time before poking the target hole), training latency

(time before entering the hidden cage) and time spent in the target quadrant were measured.

### 5.2. Quantification of Aβ1-42 and Aβ1-40

ELISA were performed only in 8-mo mice. All the steps were performed in LoBind tubes to limit loss of amyloid peptides. Homogenization Buffer (HB) was 50 mM Tris-HCl (sigma, T2788), 1X Protease Inhibitor (ThermoFisher, A32961), 150 mM NaCl (Sigma, S5886), 1% Triton X-100 (Sigma, 066 K0089), pH 7.4. Cortex were weighted and the ratio tissue/ HB adjusted to 2.5 μg/ml. Samples were sonicated (7 pulses, 40% amplitude) in HB then centrifuged at 17,500 g, 4 °C for 20 min. Protein concentration in the supernatant (soluble fraction) was determined using BCA technique, and adjusted to 0.2 μg/μl using MSD Diluent 35. For Aβ species detection, the MSD multiplex Aβ 6E10 kit (MSD, K15200E) protocol was followed. Briefly, wells were incubated with Diluent 35 at RT for 1 h under agitation, then rinsed 3 times with 0.05% Tween-20 containing PBS (Washing Solution, WS). In each well, the Detection Solution (2% 6E10, 1% $A\beta_{1\text{-}40}$ blocker in Diluent 100) was added, followed by the samples. After 2 h incubation at RT under agitation, the wells were rinsed 3 times with the WS. Finally, 2X Read Buffer T was added and the plate was read on a MESO QuickPlex SQ 120 plate reader.

## Funding

This work was supported by funding from France Alzheimer (Grant AAP 2013 _ MicroMalzh). The PhD funding of J. Hua was supported by the Labex ICST (ANR 11-LABX-0015).

## Acknowledgements

We acknowledge Leportier M. and Dr Mesbah K. (RAM-iExplore plateform) for help with animal breeding; the imaging facility MRI (Dr Cau J.), member of the national infrastructure France-BioImaging infrastructure supported by the French National Research Agency (ANR-10-INBS-04, «Investments for the future») for help with immunohistochemistry quantification; Drs Tiers L. and Lehmann S. (Laboratory of Biochemistry – Clinical Proteomic (LBPC) for help with MSD quantification. Drs Pisa L., Pastore M. and Reynes C. (StatAbio plateform, BCM, Univ. Montpellier, CNRS, INSERM, Montpellier, France) for useful advice on statistical analyses.

## Appendix A. Supplementary data

Supplementary data to this article can be found online at https://doi.org/10.1016/j.bbi.2020.10.021.

## References

Arnoux, I., Audinat, E., 2015. Fractalkine Signaling and microglia functions in the developing brain. Neural Plast. 2015, 689404 https://doi.org/10.1155/2015/689404.

Baik, S.H., Kang, S., Son, S.M., Mook-Jung, I., 2016. Microglia contributes to plaque growth by cell death due to uptake of amyloid beta in the brain of Alzheimer's disease mouse model. Glia 64, 2274–2290. https://doi.org/10.1002/glia.23074.

Bedner, P., Dupper, A., Huttmann, K., Muller, J., Herde, M.K., Dublin, P., Deshpande, T., Schramm, J., Haussler, U., Haas, C.A., Henneberger, C., Theis, M., Steinhauser, C., 2015. Astrocyte uncoupling as a cause of human temporal lobe epilepsy. Brain 138, 1208–1222. https://doi.org/10.1093/brain/awv067.

Bellenguez, C., Grenier-Boley, B., Lambert, J.C., 2020. Genetics of Alzheimer's disease: where we are, and where we are going. Curr. Opin. Neurobiol. 61, 40–48. https://doi.org/10.1016/j.conb.2019.11.024.

Bhaskar, K., Hobbs, G.A., Yen, S.H., Lee, G., 2010. Tyrosine phosphorylation of tau accompanies disease progression in transgenic mouse models of tauopathy. Neuropathol. Appl. Neurobiol. 36, 462–477. https://doi.org/10.1111/j.1365-2990.2010.01103.x.

Bordeleau, M., Carrier, M., Luheshi, G.N., Tremblay, M.E., 2019. Microglia along sex lines: From brain colonization, maturation and function, to implication in neurodevelopmental disorders. Semin. Cell Dev. Biol. 94, 152–163. https://doi.org/10.1016/j.semcdb.2019.06.001.

Cho, S.H., Sun, B., Zhou, Y., Kauppinen, T.M., Halabisky, B., Wes, P., Ransohoff, R.M., Gan, L., 2011. CX3CR1 protein signaling modulates microglial activation and protects against plaque-independent cognitive deficits in a mouse model of Alzheimer disease. J. Biol. Chem. 286, 32713–32722. https://doi.org/10.1074/jbc.M111.254268.

Cuello, A.C., 2017. Early and late CNS inflammation in Alzheimer's disease: Two extremes of a continuum? Trends Pharmacol. Sci. 38, 956–966. https://doi.org/10.1016/j.tips.2017.07.005.

Erny, D., Hrabe de Angelis, A.L., Prinz, M., 2017. Communicating systems in the body: how microbiota and microglia cooperate. Immunology 150, 7–15. https://doi.org/10.1111/imm.12645.

Esquerda-Canals, G., Montoliu-Gaya, L., Guell-Bosch, J., Villegas, S., 2017. Mouse models of Alzheimer's disease. J. Alzheimer's Dis JAD 57, 1171–1183. https://doi.org/10.3233/JAD-170045.

Fan, Z., Brooks, D.J., Okello, A., Edison, P., 2017. An early and late peak in microglial activation in Alzheimer's disease trajectory. Brain 140, 792–803. https://doi.org/10.1093/brain/aww349.

Gallagher, J.J., Minogue, A.M., Lynch, M.A., 2013. Impaired performance of female APP/PS1 mice in the Morris water maze is coupled with increased Abeta accumulation and microglial activation. Neurodegener. Dis. 11, 33–41. https://doi.org/10.1159/000337458.

Gosselin, D., Skola, D., Coufal, N.G., Holtman, I.R., Schlachetzki, J.C.M., Sajti, E., Jaeger, B.N., O'Connor, C., Fitzpatrick, C., Pasillas, M.P., Pena, M., Adair, A., Gonda, D.D., Levy, M.L., Ransohoff, R.M., Gage, F.H., Glass, C.K., 2017. An environment-dependent transcriptional network specifies human microglia identity. Science 356. https://doi.org/10.1126/science.aal3222.

Guedes, J.R., Lao, T., Cardoso, A.L., El Khoury, J., 2018. Roles of microglial and monocyte chemokines and their receptors in regulating Alzheimer's disease-associated amyloid-beta and tau pathologies. Front. Neurol. 9, 549. https://doi.org/10.3389/fneur.2018.00549.

Gyoneva, S., Swanger, S.A., Zhang, J., Weinshenker, D., Traynelis, S.F., 2016. Altered motility of plaque-associated microglia in a model of Alzheimer's disease. Neuroscience 330, 410–420. https://doi.org/10.1016/j.neuroscience.2016.05.061.

Hampel, H., Caraci, F., Cuello, A.C., Caruso, G., Nistico, R., Corbo, M., Baldacci, F., Toschi, N., Garaci, F., Chiesa, P.A., Verdooner, S.R., Akman-Anderson, L., Hernandez, F., Avila, J., Emanuele, E., Valenzuela, P.L., Lucia, A., Watling, M., Imbimbo, B.P., Vergallo, A., Lista, S., 2020. A path toward precision medicine for neuroinflammatory mechanisms in Alzheimer's disease. Front. Immunol. 11, 456. https://doi.org/10.3389/fimmu.2020.00456.

Hansen, D.V., Hanson, J.E., Sheng, M., 2018. Microglia in Alzheimer's disease. J. Cell Biol. 217, 459–472. https://doi.org/10.1083/jcb.201709069.

He, C., Han, Y., Fan, Y., Deng, M., Wang, Y., 2012. Self-assembly of Abeta-based peptide amphiphiles with double hydrophobic chains. Langmuir 28, 3391–3396. https://doi.org/10.1021/la2046146.

Hebert, L.E., Weuve, J., Scherr, P.A., Evans, D.A., 2013. Alzheimer disease in the United States (2010–2050) estimated using the 2010 census. Neurology. 80, 1778–1783. https://doi.org/10.1212/WNL.0b013e31828726f5.

Heneka, M.T., Golenbock, D.T., Latz, E., 2015. Innate immunity in Alzheimer's disease. Nat. Immunol. 16, 229–236. https://doi.org/10.1038/ni.3102.

Hickman, S.E., Allison, E.K., Coleman, U., Kingery-Gallagher, N.D., El Khoury, J., 2019. Heterozygous CX3CR1 deficiency in microglia restores neuronal beta-amyloid clearance pathways and slows progression of Alzheimer's like-disease in PS1-APP mice. Front. Immunol. 10, 2780. https://doi.org/10.3389/fimmu.2019.02780.

Hickman, S.E., Allison, E.K., El Khoury, J., 2008. Microglial dysfunction and defective beta-amyloid clearance pathways in aging Alzheimer's disease mice. J. Neurosci. 28, 8354–8360. https://doi.org/10.1523/JNEUROSCI.0616-08.2008.

Hirbec, H., Marmai, C., Duroux-Richard, I., Roubert, C., Esclangon, A., Croze, S., Lachuer, J., Peyroutou, R., Rassendren, F., 2018. The microglial reaction signature revealed by RNAseq from individual mice. Glia 66, 971–986. https://doi.org/10.1002/glia.23295.

Jankowsky, J.L., Slunt, H.H., Gonzales, V., Jenkins, N.A., Copeland, N.G., Borchelt, D.R., 2004. APP processing and amyloid deposition in mice haplo-insufficient for presenilin 1. Neurobiol. Aging 25, 885–892. https://doi.org/10.1016/j.neurobiolaging.2003.09.008.

Jankowsky, J.L., Slunt, H.H., Ratovitski, T., Jenkins, N.A., Copeland, N.G., Borchelt, D.R., 2001. Co-expression of multiple transgenes in mouse CNS: a comparison of strategies. Biomol. Eng. 17, 157–165.

Janus, C., Flores, A.Y., Xu, G., Borchelt, D.R., 2015. Behavioral abnormalities in APPSwe/PS1dE9 mouse model of AD-like pathology: comparative analysis across multiple behavioral domains. Neurobiol. Aging 36, 2519–2532. https://doi.org/10.1016/j.neurobiolaging.2015.05.010.

Jiao, S.S., Bu, X.L., Liu, Y.H., Zhu, C., Wang, Q.H., Shen, L.L., Liu, C.H., Wang, Y.R., Yao, X.Q., Wang, Y.J., 2016. Sex dimorphism profile of Alzheimer's disease-type pathologies in an APP/PS1 mouse model. Neurotox. Res. 29, 256–266. https://doi.org/10.1007/s12640-015-9589-x.

Jung, S., Aliberti, J., Graemmel, P., Sunshine, M.J., Kreutzberg, G.W., Sher, A., Littman, D.R., 2000. Analysis of fractalkine receptor CX(3)CR1 function by targeted deletion and green fluorescent protein reporter gene insertion. Mol. Cell. Biol. 20, 4106–4114.

Keren-Shaul, H., Spinrad, A., Weiner, A., Matcovitch-Natan, O., Dvir-Szternfeld, R., Ulland, T.K., David, E., Baruch, K., Lara-Astaiso, D., Toth, B., Itzkovitz, S., Colonna, M., Schwartz, M., Amit, I., 2017. A unique microglia type associated with restricting development of Alzheimer's disease. Cell 169 (1276–1290), e1217. https://doi.org/10.1016/j.cell.2017.05.018.

Koenigsknecht-Talboo, J., Meyer-Luehmann, M., Parsadanian, M., Garcia-Alloza, M., Finn, M.B., Hyman, B.T., Bacskai, B.J., Holtzman, D.M., 2008. Rapid microglial

response around amyloid pathology after systemic anti-Abeta antibody administration in PDAPP mice. J. Neurosci. 28, 14156–14164. https://doi.org/10.1523/JNEUROSCI.4147-08.2008.

Lee, S., Varvel, N.H., Konerth, M.E., Xu, G., Cardona, A.E., Ransohoff, R.M., Lamb, B.T., 2010. CX3CR1 deficiency alters microglial activation and reduces beta-amyloid deposition in two Alzheimer's disease mouse models. Am. J. Pathol. 177, 2549–2562. https://doi.org/10.2353/ajpath.2010.100265.

Liu, Z., Condello, C., Schain, A., Harb, R., Grutzendler, J., 2010. CX3CR1 in microglia regulates brain amyloid deposition through selective protofibrillar amyloid-beta phagocytosis. J. Neurosci. 30, 17091–17101. https://doi.org/10.1523/jneurosci.4403-10.2010.

Lopez-Lopez, A., Gelpi, E., Lopategui, D.M., Vidal-Taboada, J.M., 2018. Association of the CX3CR1-V249I variant with neurofibrillary pathology progression in late-onset Alzheimer's disease. Mol. Neurobiol. 55, 2340–2349. https://doi.org/10.1007/s12035-017-0489-3.

Luna-Munoz, J., Peralta-Ramirez, J., Chavez-Macias, L., Harrington, C.R., Wischik, C.M., Mena, R., 2008. Thiazin red as a neuropathological tool for the rapid diagnosis of Alzheimer's disease in tissue imprints. Acta Neuropathol. 116, 507–515. https://doi.org/10.1007/s00401-008-0431-x.

Maggi, L., Scianni, M., Branchi, I., D'Andrea, I., Lauro, C., Limatola, C., 2011. CX(3)CR1 deficiency alters hippocampal-dependent plasticity phenomena blunting the effects of enriched environment. Front. Cell. Neurosci. 5, 22. https://doi.org/10.3389/fncel.2011.00022.

Miller, B.C., Eckman, E.A., Sambamurti, K., Dobbs, N., Chow, K.M., Eckman, C.B., Hersh, L.B., Thiele, D.L., 2003. Amyloid-beta peptide levels in brain are inversely correlated with insulysin activity levels in vivo. Proc. Natl. Acad. Sci. USA 100, 6221–6226. https://doi.org/10.1073/pnas.1031520100.

Minkeviciene, R., Ihalainen, J., Malm, T., Matilainen, O., Keksa-Goldsteine, V., Goldsteins, G., Iivonen, H., Leguit, N., Glennon, J., Koistinaho, J., Banerjee, P., Tanila, H., 2008. Age-related decrease in stimulated glutamate release and vesicular glutamate transporters in APP/PS1 transgenic and wild-type mice. J. Neurochem. 105, 584–594. https://doi.org/10.1111/j.1471-4159.2007.05147.x.

Niu, H., Alvarez-Alvarez, I., Guillen-Grima, F., Aguinaga-Ontoso, I., 2017. Prevalence and incidence of Alzheimer's disease in Europe: A meta-analysis. Neurologia 32, 523–532. https://doi.org/10.1016/j.nrl.2016.02.016.

Nordengen, K., Kirsebom, B.E., Henjum, K., Selnes, P., Gisladottir, B., Wettergreen, M., Torsetnes, S.B., Grontvedt, G.R., Waterloo, K.K., Aarsland, D., Nilsson, L.N.G., Fladby, T., 2019. Glial activation and inflammation along the Alzheimer's disease continuum. J. Neuroinflamm. 16, 46. https://doi.org/10.1186/s12974-019-1399-2.

Orre, M., Kamphuis, W., Osborn, L.M., Jansen, A.H., Kooijman, L., Bossers, K., Hol, E.M., 2014. Isolation of glia from Alzheimer's mice reveals inflammation and dysfunction. Neurobiol. Aging 35, 2746–2760. https://doi.org/10.1016/j.neurobiolaging.2014.06.004.

Reshef, R., Kreisel, T., Beroukhim Kay, D., Yirmiya, R., 2014. Microglia and their CX3CR1 signaling are involved in hippocampal- but not olfactory bulb-related memory and neurogenesis. Brain Behav. Immun. 41, 239–250. https://doi.org/10.1016/j.bbi.2014.04.009.

Rogers, J.T., Morganti, J.M., Bachstetter, A.D., Hudson, C.E., Peters, M.M., Grimmig, B.A., Weeber, E.J., Bickford, P.C., Gemma, C., 2011. CX3CR1 deficiency leads to impairment of hippocampal cognitive function and synaptic plasticity. J. Neurosci. 31, 16241–16250. https://doi.org/10.1523/JNEUROSCI.3667-11.2011.

Sellner, S., Paricio-Montesinos, R., Spiess, A., Masuch, A., Erny, D., Harsan, L.A., Elverfeldt, D.V., Schwabenland, M., Biber, K., Staszewski, O., Lira, S., Jung, S., Prinz, M., Blank, T., 2016. Microglial CX3CR1 promotes adult neurogenesis by inhibiting Sirt 1/p65 signaling independent of CX3CL1. Acta Neuropathol. Commun. 4, 102. https://doi.org/10.1186/s40478-016-0374-8.

Takatori, S., Wang, W., Iguchi, A., Tomita, T., 2019. Genetic risk factors for Alzheimer disease: emerging roles of microglia in disease pathomechanisms. Adv. Exp. Med. Biol. 1118, 83–116. https://doi.org/10.1007/978-3-030-05542-4_5.

Thion, M.S., Low, D., Silvin, A., Chen, J., Grisel, P., Schulte-Schrepping, J., Blecher, R., Ulas, T., Squarzoni, P., Hoeffel, G., Coulpier, F., Siopi, E., David, F.S., Scholz, C., Shihui, F., Lum, J., Amoyo, A.A., Larbi, A., Poidinger, M., Buttgereit, A., Lledo, P.M., Greter, M., Chan, J.K.Y., Amit, I., Beyer, M., Schultze, J.L., Schlitzer, A., Pettersson, S., Ginhoux, F., Garel, S., 2018. Microbiome Influences prenatal and adult microglia in a sex-specific manner. Cell 172 (500–516), e516. https://doi.org/10.1016/j.cell.2017.11.042.

van der Kant, R., Goldstein, L.S.B., Ossenkoppele, R., 2020. Amyloid-beta-independent regulators of tau pathology in Alzheimer disease. Nat. Rev. Neurosci. 21, 21–35. https://doi.org/10.1038/s41583-019-0240-3.

Verheijen, J., Sleegers, K., 2018. Understanding Alzheimer disease at the interface between genetics and transcriptomics. Trends Genet. 34, 434–447. https://doi.org/10.1016/j.tig.2018.02.007.

Vina, J., Lloret, A., 2010. Why women have more Alzheimer's disease than men: gender and mitochondrial toxicity of amyloid-beta peptide. J. Alzheimer's Dis JAD 20 (Suppl 2), S527–S533. https://doi.org/10.3233/JAD-2010-100501.

Wang, J., Tanila, H., Puolivali, J., Kadish, I., van Groen, T., 2003. Gender differences in the amount and deposition of amyloidbeta in APPswe and PS1 double transgenic mice. Neurobiol. Dis. 14, 318–327. https://doi.org/10.1016/j.nbd.2003.08.009.

Wolf, Y., Yona, S., Kim, K.W., Jung, S., 2013. Microglia, seen from the CX3CR1 angle. Front. Cell. Neurosci. 7, 26. https://doi.org/10.3389/fncel.2013.00026.

Zhang, M., Xu, G., Liu, W., Ni, Y., Zhou, W., 2012. Role of fractalkine/CX3CR1 interaction in light-induced photoreceptor degeneration through regulating retinal microglial activation and migration. PLoS One 7, e35446. https://doi.org/10.1371/journal.pone.0035446.

Zhou, C.N., Chao, F.L., Zhang, Y., Jiang, L., Zhang, L., Luo, Y.M., Xiao, Q., Chen, L.M., Tang, Y., 2018. Sex differences in the white matter and myelinated fibers of APP/PS1 mice and the effects of running exercise on the sex differences of AD mice. Front. Aging Neurosci. 10, 243. https://doi.org/10.3389/fnagi.2018.00243.

Zujovic, V., Schussler, N., Jourdain, D., Duverger, D., Taupin, V., 2001. In vivo neutralization of endogenous brain fractalkine increases hippocampal TNFalpha and 8-isoprostane production induced by intracerebroventricular injection of LPS. J. Neuroimmunol. 115, 135–143. https://doi.org/10.1016/s0165-5728(01)00259-4.